Neurochemistry International 122 (2019) 8–18

Contents lists available at ScienceDirect

Neurochemistry International

journal homepage: www.elsevier.com/locate/neuint

Balance between dopamine and adenosine signals regulates the PKA/Rap1 pathway in striatal medium spiny neurons

Xinjian Zhang[a], Taku Nagai[b,**], Rijwan Uddin Ahammad[a], Keisuke Kuroda[a], Shinichi Nakamuta[a], Takashi Nakano[c], Naoto Yukinawa[d], Yasuhiro Funahashi[a], Yukie Yamahashi[a], Mutsuki Amano[a], Junichiro Yoshimoto[c,d], Kiyofumi Yamada[b], Kozo Kaibuchi[a,*]

[a] Department of Cell Pharmacology, Graduate School of Medicine, Nagoya University, Nagoya, Aichi, 466-8550, Japan
[b] Department of Neuropsychopharmacology and Hospital Pharmacy, Graduate School of Medicine, Nagoya University, Nagoya, Aichi, 466-8550, Japan
[c] Graduate School of Information Science, Nara Institute of Science and Technology, Ikoma, Nara, 630-0192, Japan
[d] Neural Computation Unit, Okinawa Institute of Science and Technology Graduate University, Onna, Okinawa, 904-0495, Japan

ARTICLE INFO

Keywords:
Dopamine
Adenosine
Striatum
Medium spiny neuron
PKA
Rap1gap

ABSTRACT

Medium spiny neurons (MSNs) expressing dopamine D1 receptor (D1R) or D2 receptor (D2R) are major components of the striatum. Stimulation of D1R activates protein kinase A (PKA) through G_{olf} to increase neuronal activity, while D2R stimulation inhibits PKA through G_i. Adenosine A2A receptor (A2AR) coupled to G_{olf} is highly expressed in D2R-MSNs within the striatum. However, how dopamine and adenosine co-operatively regulate PKA activity remains largely unknown. Here, we measured Rap1gap serine 563 phosphorylation to monitor PKA activity and examined dopamine and adenosine signals in MSNs. We found that a D1R agonist increased Rap1gap phosphorylation in striatal slices and in D1R-MSNs *in vivo*. A2AR agonist CGS21680 increased Rap1gap phosphorylation, and pretreatment with the D2R agonist quinpirole blocked this effect in striatal slices. D2R antagonist eticlopride increased Rap1gap phosphorylation in D2R-MSNs *in vivo*, and the effect of eticlopride was blocked by the pretreatment with the A2AR antagonist SCH58261. These results suggest that adenosine positively regulates PKA in D2R-MSNs through A2AR, while this effect is blocked by basal dopamine *in vivo*. Incorporating computational model analysis, we propose that the shift from D1R-MSNs to D2R-MSNs or vice versa appears to depend predominantly on a change in dopamine concentration.

1. Introduction

In the brain, dopamine functions as a neuromodulator and is associated with motor function, motivation, learning and reward (Wise, 2004; Beaulieu and Gainetdinov, 2011). Several neuropsychological diseases are associated with dysfunctions of the dopaminergic system including Parkinson's disease, schizophrenia, drug addiction, attention deficit hyperactivity disorder and restless legs syndrome (Allen, 2004; Iversen and Iversen, 2007; Pascoli et al., 2015). There are various dopaminergic pathways in the brain. Two major pathways are the mesolimbic pathway and nigrostriatal pathway, which project dopamine neurons from the substantia nigra and the ventral tegmental area to the striatum including the nucleus accumbens (NAc). The striatum is a subcortical part of the forebrain and interacts with the cerebral cortex and thalamus, resulting in various behavioral consequences, including not only body movements but also motivation and learning (Shohamy, 2011).

Striatal medium spiny neurons (MSNs) are major components of the basal ganglia, which make up approximately 95% of neurons within the striatum, and receive dopaminergic regulation (Kemp and Powell, 1971). MSNs are classified into two types: MSNs expressing the dopamine D1 receptor (D1R-MSNs) or dopamine D2 receptor (D2R-MSNs) (Gerfen et al., 1990). In the NAc, D1R-MSNs are involved in rewarding behavior, while D2R-MSNs are involved in aversive behavior (Hikida et al., 2010). D1R is coupled to G_{olf}, whose stimulation activates protein kinase A (PKA) through adenylate cyclase (AC) (Herve et al., 1993, 2001). On the other hand, D2R is coupled to G_i, whose activation results in an inhibition of the cAMP/PKA signaling pathway (Montmayeur

* Corresponding author. Department of Cell Pharmacology, Graduate School of Medicine, Nagoya University, 65 Tsurumai-cho, Showa-ku, Nagoya, Aichi, 466-8550, Japan.
** Corresponding author. Department of Neuropsychopharmacology and Hospital Pharmacy, Graduate School of Medicine, Nagoya University, 65 Tsurumai-cho, Showa-ku, Nagoya, Aichi, 466-8550, Japan.
E-mail addresses: t-nagai@med.nagoya-u.ac.jp (T. Nagai), kaibuchi@med.nagoya-u.ac.jp (K. Kaibuchi).

https://doi.org/10.1016/j.neuint.2018.10.008
Received 27 June 2018; Received in revised form 2 October 2018; Accepted 3 October 2018
Available online 15 October 2018
0197-0186/ © 2018 The Authors. Published by Elsevier Ltd. This is an open access article under the CC BY license (http://creativecommons.org/licenses/BY/4.0/).

et al., 1993). *In vivo* imaging of transgenic mice expressing a PKA fluorescence resonance energy transfer biosensor revealed that cocaine administration increases PKA activity in D1R-MSNs of the striatum, whereas PKA activity is decreased in D2R-MSNs (Goto et al., 2015), indicating that PKA activity is reciprocally regulated between D1R-MSNs and D2R-MSNs by extracellular dopamine. Thus, activity of the basal ganglia is controlled by the dynamic balance between D1R-MSNs and D2R-MSNs.

To elucidate the mode of action of dopamine in MSNs, Paul Greengard's group has investigated the cAMP/PKA-dependent signaling pathway and found that dopamine- and cAMP-regulated phosphoprotein of 32-kDa (DARPP-32) and α-amino-3-hydroxy-5-methyl-4-isoxazolepropionic acid (AMPA)-selective glutamate receptor 1 (GluR1) act as PKA substrates and are involved in synaptic plasticity (Walaas et al., 1983; Snyder et al., 2000). N-methyl-D-aspartate (NMDA) receptor subunit1 (NR1) is also known to be the PKA substrate (Tingley et al., 1997). DARPP-32 has been reported to amplify the action of dopamine in MSNs. When DARPP-32 is phosphorylated by PKA, it can inhibit protein phosphatase-1 activity and sustain the phosphorylated state of the protein (Nishi et al., 2011). Both GluR1 and NR1 phosphorylations are implied to increase the expression level of surface AMPA receptors and NMDA receptors (Esteban et al., 2003; Hallett et al., 2006). McAvoy et al. (2009) have reported that PKA phosphorylates Rap1gap at serine 563 (serine 499 in the human Rap1gap isoform) in striatal slices, and the phosphorylation of Rap1gap leads to the inactivation of its GTPase-activating protein (GAP) activity. We have recently carried out a comprehensive phosphoproteomic analysis of PKA substrates downstream of D1R and identified novel PKA substrates including Rasgrp2 (Nagai et al., 2016a). Rasgrp2 is a guanine nucleotide exchange factor (GEF) for Rap1 that can activate Rap1 signaling to regulate neuronal excitability and cocaine-induced reward responses by acting through the MAPKK/MAPK pathway (Nagai et al., 2016b). In addition to Rasgrp2, we have also found that, among the putative PKA substrates, Rap1gap is phosphorylated by D1R agonist (Nagai et al., 2016a). These findings suggest that D1R/PKA/Rap1gap is another signaling pathway for dopamine action to control Rap1 activity *in vivo* (Fig. 1a). The phosphorylation of Rap1gap appears to be useful for monitoring PKA activity in striatal MSNs. However, whether dopamine D1R stimulation promotes phosphorylation of Rap1gap *in vivo* remains unclear.

Dopamine suppresses neuronal activity through D2R (Gerfen and Surmeier, 2011), whereas other neurotransmitters or neuromodulators appear to increase the activity of D2R-MSNs. One such neuromodulator implicated to increase the D2R-MSN activity is adenosine, which is one of the prominent neuromodulators in the striatum. In the central nervous system, adenosine serves as a neuromodulator involved in sleep regulation, neuroprotection, locomotion, and blood flow regulation (Morgan et al., 1991; Dunwiddie and Masino, 2001; Porkka-Heiskanen et al., 2002; Wardas, 2002). Adenosine exerts its effects through adenosine receptors: adenosine A1 receptor (A1R), adenosine A2A receptor (A2AR), adenosine A2B receptor and adenosine A3 receptor. A1R is widely distributed in the central nervous system, while A2Rs are located mainly in the striatum and olfactory bulb (Wardas, 2002; Porkka-Heiskanen et al., 2002). In the striatum, D2R-MSNs express A2AR, which couples to the G_{olf} protein, whereas D1R-MSNs express A1R, which couples to the G_i protein (Fink et al., 1992; Ferre et al., 1996; Fredholm et al., 2000; Kull et al., 2000). Thus, PKA activity in D2R-MSNs is speculated to be positively controlled by adenosine/A2AR and negatively by dopamine/D2R. However, how these two pathways cooperatively act in D2R-MSNs remains largely unknown. Notably, A2AR and D2R in MSNs are highlighted as therapeutic targets for Parkinson's disease and schizophrenia (Richardson et al., 1997; Kapur and Remington, 2001; Seeman, 2013; Pinna, 2014).

In light of these observations, we here investigated the modes of action of dopamine and adenosine signal towards Rap1gap phosphorylation in D2R-MSNs by use of striatal slice, *in vivo*, and computational model analyses. We found that adenosine stimulated Rap1gap phosphorylation through A2AR in striatal slice. *In vivo* analysis showed that Rap1gap phosphorylation was positively regulated by adenosine/A2AR, and this effect was counteracted by dopamine/D2R. The mathematical model revealed that the balance of adenosine/A2AR and dopamine/D2R regulated Rap1gap phosphorylation in D2R-MSNs.

2. Material & methods

2.1. Animals

Male C57BL/6 mice (21–26 g) at the age of 7 weeks were purchased from Japan SLC, Inc. (Shizuoka, Japan). Mice were housed in a density of four mice per cage (17 cm wide × 28 cm long × 13 cm high) in the specific pathogen-free animal facility under standard conditions (23 ± 1 °C, 50 ± 5% humidity) with a 12-h light/dark cycle. Food and water were available *ad libitum*. Generation of *Drd1-mVenus* and *Drd2-mVenus* transgenic mice were described previously (Nagai et al., 2016a). Transgenic mice expressing a variant of yellow fluorescent protein (mVenus) under the control of D1R promoter (Drd1-mVenus, RBRC03111, Riken BRC, Tsukuba, Japan) or D2R promoter (Drd2-mVenus, RBRC02332, Riken BRC) were identified by PCR with genomic DNA prepared from tail clips. All mice were randomly assigned into control and experimental groups using a completely randomized digital table made by Microsoft Excel. All animal experiments were pre-registered, approved (approved number 29385) and performed in the laboratory in accordance with the guidelines for the care and use of laboratory animals established by the Animal Experiments Committee of Nagoya University Graduate School of Medicine.

2.2. Drugs

CGS21680, S-(−)-Eticlopride hydrochloride and (±)-quinpirole dihydrochloride were purchased from Sigma-Aldrich Co. (St. Louis, MO, USA). SKF81297 hydrobromide and SCH58261 were purchased from Tocris Bioscience (Bristol, UK). Eticlopride, quinpirole and SKF81297 were dissolved in sterile distilled water (DW) or saline. CGS21680 and SCH58261 were dissolved in DMSO as a stock solution and diluted in saline to the final concentration. The dosages of drugs used in the present study were chosen from previous reports (Svenningsson et al., 2000).

2.3. Antibodies

Rabbit polyclonal antibody against Rap1gap phosphorylated at serine 563 (S563) was produced against the phosphopeptide CGSRRSpS^{563}AIGIE. The obtained antiserum was then affinity-purified against the phosphoprotein on membranes as previously described with some modification (Kuroda et al., 2011). In brief, GST-hRap1gap-411-681aa protein was purified from *E. coli* as antigen described previously (Kato et al., 2012) and was subjected to *in vitro* phosphorylation assay using PKA (Hamaguchi et al., 2015). Non-phosphorylated and phosphorylated antigens were applied to SDS-PAGE and transferred to membranes separately. The antiserum was precleared by incubating antiserum with membranes bound with the non-phosphorylated antigen. The precleared antiserum was collected and incubated with membranes bound with the phosphorylated antigen. After incubation, antibody that bound with the phosphorylated antigen was eluted with 200 μl 0.1 M glycine-HCl (pH 2.5), and pH was adjusted to 7.5. The following antibodies were obtained commercially: rabbit anti-phospho-GluR1 (S845) (RRID: AB_10860773), rabbit anti-phospho-NMDAR1 (S897) (RRID: AB_2112139), and rabbit anti-phospho-DARPP-32 (threonine 34) (T34) (RRID: AB_2169004) from Cell Signaling Technology (Danvers, MA, USA); mouse anti-GluR1 (RRID: AB_11212678) from Millipore (Billerica, MA, USA); mouse anti-NMDAR1 (RRID: AB_396353) and mouse anti-DARPP-32 (RRID: AB_398980) from BD

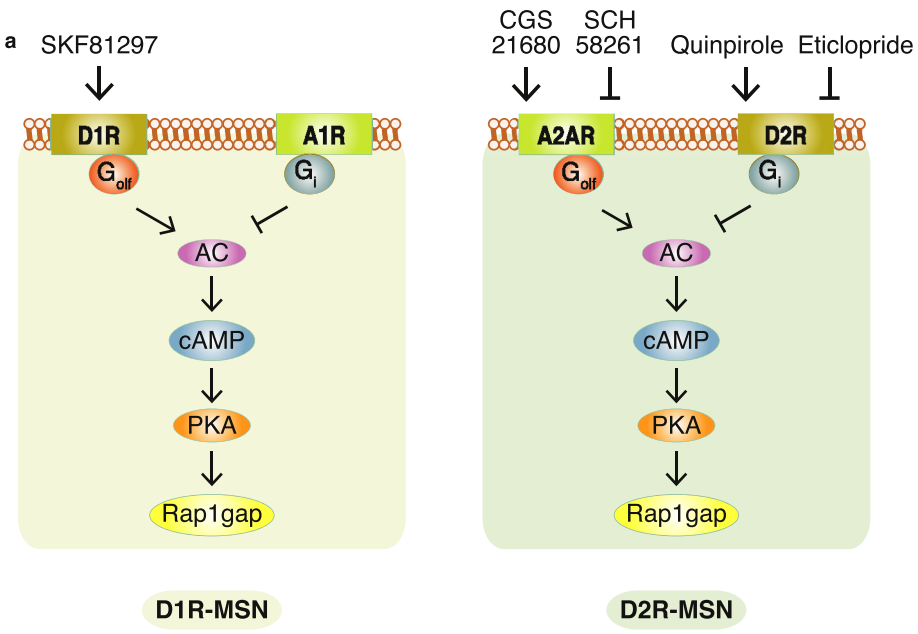

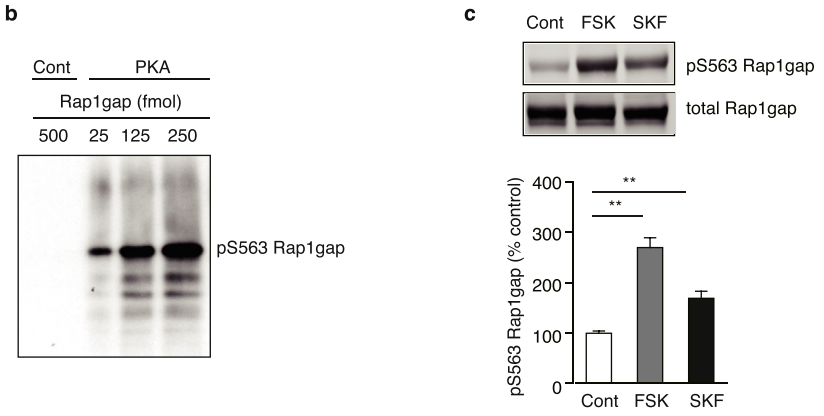

Fig. 1. Stimulation of the dopamine D1R promotes Rap1gap phosphorylation in striatal slices. **(a)** Model of DR and AR signaling pathways in D1R-MSN and D2R-MSN. **(b)** Specificity of the antibody against Rap1gap phosphorylated by PKA. Five hundred fmol of GST-Rap1gap-411-681 aa containing the indicated amount of phosphorylated or non-phosphorylated protein was subjected to SDS-PAGE, followed by immunoblot analysis with the anti-Rap1gap pS563 antibody. **(c)** Forskolin (FSK) and SKF81279 (SKF) stimulated the phosphorylation of Rap1gap in striatal slices. Striatal slices were treated with either FSK (1 μM) or SKF (1 μM) for 10 min. Rap1gap phosphorylation was measured via immunoblotting using antibodies that were specific for total Rap1gap or for Rap1gap phosphorylated at S563. Upper panels show representative immunoblots. Quantification of the immunoblotting assay is shown in the bottom panel. Data are presented as the mean ± SEM (n = 10 slices for control (cont), n = 6 slices for FSK, n = 10 slices for SKF) of three independent experiments. One-way ANOVA analysis, $F(2,23) = 40.22$, $p < 0.01$. **$p < 0.01$ compared with the cont. Full-length blots are presented in Supplementary Fig. S6.

Bioscience (Franklin Lakes, NJ, USA); rabbit anti-Rap1gap (RRID: AB_777621) from Abcam (Cambridge, UK); rat anti-GFP antibody (RRID: AB_10013361) from Nacalai Tesque (Kyoto, Japan); goat anti-rat Alexa Fluor 488 (RRID: AB_2534074), goat anti-rabbit Alexa Fluor 568 (RRID:AB_143157) and goat anti-rabbit Alexa Fluor 680 (RRID: AB_10375714) from Thermo Fisher Scientific (Waltham, MA, USA); and goat anti-mouse IRDye 800CW (RRID: AB_621842) from LI-COR Biosciences (Lincoln, NE, USA).

2.4. Preparation of striatal slices

Striatal slices were prepared from male C57BL/6 mice as described previously (Nishi et al., 1997). The brain was removed and kept in Krebs-HCO_3^- buffer (124 mM NaCl, 4 mM KCl, 26 mM $NaHCO_3$, 1.5 mM $CaCl_2$, 1.25 mM KH_2PO_4, 1.5 mM $MgSO_4$, and 10 mM D-glucose, pH 7.4). Coronal brain slices (350 μm) were prepared using a VT1200S vibratome (Leica Microsystems, Wetzlar, Germany). After isolation of the whole striatum from the brain slice, striatal slices were incubated at 30 °C in Krebs-HCO_3^- buffer with 10 μg/ml adenosine deaminase for 30 min under constant oxygenation with 95% O_2/5% CO_2. The buffer was replaced with fresh Krebs-HCO_3^- buffer and preincubated for 30 min. Slices were treated with SKF81297 (1 μM) or forskolin (1 μM) for 10 min. Striatal slices were pretreated with quinpirole (1 μM) 10 min before the 5 min treatment with CGS21680 (5 μM). After treatment with drugs, slices were kept in liquid nitrogen and stored in a freezer at −80 °C until assayed. Samples were homogenized in 1% SDS buffer. Protein concentration was measured by BCA assay. Proteins (20 μg) were applied in each point for immunoblotting.

2.5. Tissue preparation for immunoblotting

Mice were injected intraperitoneally (i.p.) with drugs (CGS21680 dissolved in 0.2% DMSO, SKF81297 dissolved in saline, or eticlopride dissolved in saline) or their corresponding vehicle (saline or 0.2% DMSO in saline) and sacrificed by decapitation 15 min later. SCH58261 dissolved in 1.4% DMSO was administered 5 min before eticlopride treatment. After the decapitation, the heads of the mice were immediately immersed into liquid nitrogen for 4 s, and the brains were removed. The NAc was dissected out on an ice-cold plate. Each tissue sample was snap frozen in liquid nitrogen and stored in a freezer at −80 °C until assayed for immunoblotting.

2.6. Immunoblotting

For immunoblotting, 20 μg protein of each sample was loaded on 10% acrylamide gels. Then, the proteins were separated through gel electrophoresis and transferred from the gel onto a polyvinylidene difluoride membrane. Membranes were blocked for 1 h with Blocking-One (Nacalai Tesque) and incubated overnight at 4 °C with primary antibodies anti-phospho-GluR1 (S845) (1:1000), anti-GluR1 (1:1000),

anti-phospho-NMDAR1 (S897) (1:1000), anti-NMDAR1 (1:1000), anti-phospho-DARPP-32 (T34) (1:1000), anti-DARPP-32 (1:1000), anti-phospho-Rap1gap (S563) (1:1000) and anti-Rap1gap (1:10000). After the membranes were washed, they were incubated with goat anti-rabbit Alexa Fluor 680 or goat anti-mouse IRDye 800CW at room temperature for 1 h. Antibody binding was detected using an infrared imaging system (LI-COR Biosciences). Band intensities were quantified using ImageStudio software (LI-COR Biosciences).

2.7. Immunohistochemistry

Mice were anesthetized with tribromoethanol (200 mg/kg, i.p.) for rapid and deep anesthesia and transcardially perfused with isotonic 4% paraformaldehyde. Then, the brains were removed and incubated in 4% paraformaldehyde overnight at 4 °C. The brains were cryoprotected in 20–30% sucrose in PBS. Then, the brains were frozen using O.C.T compound (Sakura Finetechnical, Tokyo, Japan). The coronal striatal sections (20 μm-thick) were fixed with 4% paraformaldehyde for 5 min and incubated with 0.3% Triton X-100/PBS for 10 min. After the slices were washed with PBS for 10 min twice, the slices were incubated for 1 h at room temperature in blocking buffer (5% normal goat serum/0.3% Triton X-100/PBS) and overnight at 4 °C in the presence of the primary antibodies (anti-GFP antibody, 1:1000; anti-phospho-Rap1gap (S563) antibody, 1:500). Sections were washed three times with PBS and incubated with the secondary antibodies (goat anti-rat Alexa Fluor 488, 1:1000; goat anti-rabbit Alexa Fluor 568, 1:1000) in 0.3% Triton X-100/PBS for 1 h at RT. After the slices were washed with PBS, they were mounted on slide glasses and observed using a confocal microscope (LSM780, Carl Zeiss, Jena, Germany).

2.8. Mathematical modeling

A signaling pathway model of D2R-MSNs was constructed based on previous modeling studies (Nakano et al., 2010; Nair et al., 2015) to reproduce the interaction between the dopamine and adenosine signals. The biochemical reaction in the model can be written by differential equations. For example, the binding reaction of A and B produces molecule AB as the following differential equation:

$$\frac{d[AB]}{dt} = k_f[A][B] - k_b[AB],$$

where k_f and k_b are the rate constants of forward and backward reactions. The affinity parameters of adenosine/A2AR and dopamine/D2R were set according to the experimentally determined kinetic constants provided by the IUPHAR database (Southan et al., 2016) and the previous models (Nakano et al., 2010; Nair et al., 2015). The differential equations were numerically calculated using the COPASI simulator (Hoops et al., 2006).

2.9. Experimental design and statistical analysis

Assumptions of how well normality and equal variances fit the data could not be reliably assessed because of the small sample sizes. Sample size was not predetermined by formal power analysis statistical methods. No samples or data were excluded from the analysis. Data analysis was performed using Prism 6 Statistics software (GraphPad Software, Inc., La Jolla, USA). All data are expressed as the means ± SEM. A one-way, two-way, or three-way analysis of variance (ANOVA) was used, followed by Tukey's test when the F ratios were significant ($p < 0.05$). The number of animals and brain slices are indicated in the text and figure legends.

3. Results

3.1. Stimulation of dopamine D1R promotes Rap1gap phosphorylation in striatal slices

PKA has been shown to phosphorylate Rap1gap at S563 (McAvoy et al., 2009). Consistently, our previous phosphoproteomic analysis of D1R signaling showed that Rap1gap is phosphorylated at S563 in striatal slices after treatment with the dopamine D1R agonist SKF81297 (Fig. 1a) (Nagai et al., 2016a). Based on these findings, we developed an antibody against Rap1gap phosphorylated at S563 and confirmed that this antibody specifically recognized phosphorylated Rap1gap by PKA without cross-reacting with the non-phosphorylated Rap1gap (Fig. 1b and Fig. S11a). We next examined whether SKF81297 and forskolin, an inducer of cAMP, enhanced the phosphorylation of Rap1gap in striatal slices using the phospho-specific antibody (Fig. S1). The phosphorylation level of Rap1gap at S563 was significantly increased after the treatment of the striatal slice with SKF81297 or forskolin compared with that of control ($p < 0.01$, Fig. 1c), indicating that D1R and PKA stimulation promotes Rap1gap phosphorylation at S563 (Fig. 1a).

3.2. Stimulation of adenosine A2AR promotes Rap1gap phosphorylation in striatal slices

To monitor Rap1gap phosphorylation in D2R-MSNs, striatal slices were treated with the A2AR agonist CGS21680 and D2R agonist quinpirole (Fig. 1a and Fig. S2). Treatment of striatal slices with CGS21680 significantly increased the phosphorylation level of Rap1gap at S563 ($p < 0.01$, Fig. 2a). The CGS21680-stimulated phosphorylation of Rap1gap at S563 was completely blocked by pretreatment with quinpirole, whereas quinpirole itself had no effect on Rap1gap phosphorylation ($p < 0.01$, Fig. 2a). We also confirmed the PKA activity using other well-known PKA substrates, including DARPP-32 (Lindskog et al., 1999; Yabuuchi et al., 2006), AMPA receptor GluR1 subunit (Snyder et al., 2000), and NMDA receptor NR1 subunit (Tingley et al., 1997). Treatment of the slices with CGS21680 increased phosphorylation levels of DARPP-32 at T34 ($p < 0.01$, Fig. 2b), AMPA receptor GluR1 subunit at S845 ($p < 0.01$, Fig. 2c), and NMDA receptor NR1 subunit at S897 ($p < 0.01$, Fig. 2d). Pretreatment of slices with quinpirole blocked the CGS21680-induced phosphorylation of these proteins ($p < 0.01$, Fig. 2b–d). These results suggest that A2AR but not D2R stimulation promotes Rap1gap phosphorylation in striatal slices, and that the phosphorylation of Rap1gap is a useful molecular marker to monitor PKA activity.

3.3. Stimulation of dopamine D1R promotes Rap1gap phosphorylation in the accumbal D1R-MSNs

To investigate the regulatory effect of D1R on Rap1gap phosphorylation *in vivo*, we examined the phosphorylation level of Rap1gap in the NAc of C57BL/6 mice by immunoblotting (Fig. S3a). The phosphorylation level of Rap1gap at S563 was significantly increased in the SKF81297-treated mice ($p < 0.05$, Fig. 3a). We also immunohistochemically investigated if SKF81297 stimulates phosphorylation of Rap1gap in accumbal D1R-MSNs by treating *Drd1-mVenus* transgenic mice, which express mVenus in the D1R-MSNs, with SKF81297 (Fig. S3b). SKF81297 treatment increased the number of phosphorylated Rap1gap-positive cells, and most of the signals were colocalized with mVenus-positive cells in the NAc of *Drd1-mVenus* transgenic mice (Fig. 3b). There were few cells positive for Rap1gap phosphorylation in saline-treated mice (Fig. 3b). These results indicate that D1R stimulation increased PKA activity in the accumbal D1R-MSNs *in vivo* (Fig. 1a).

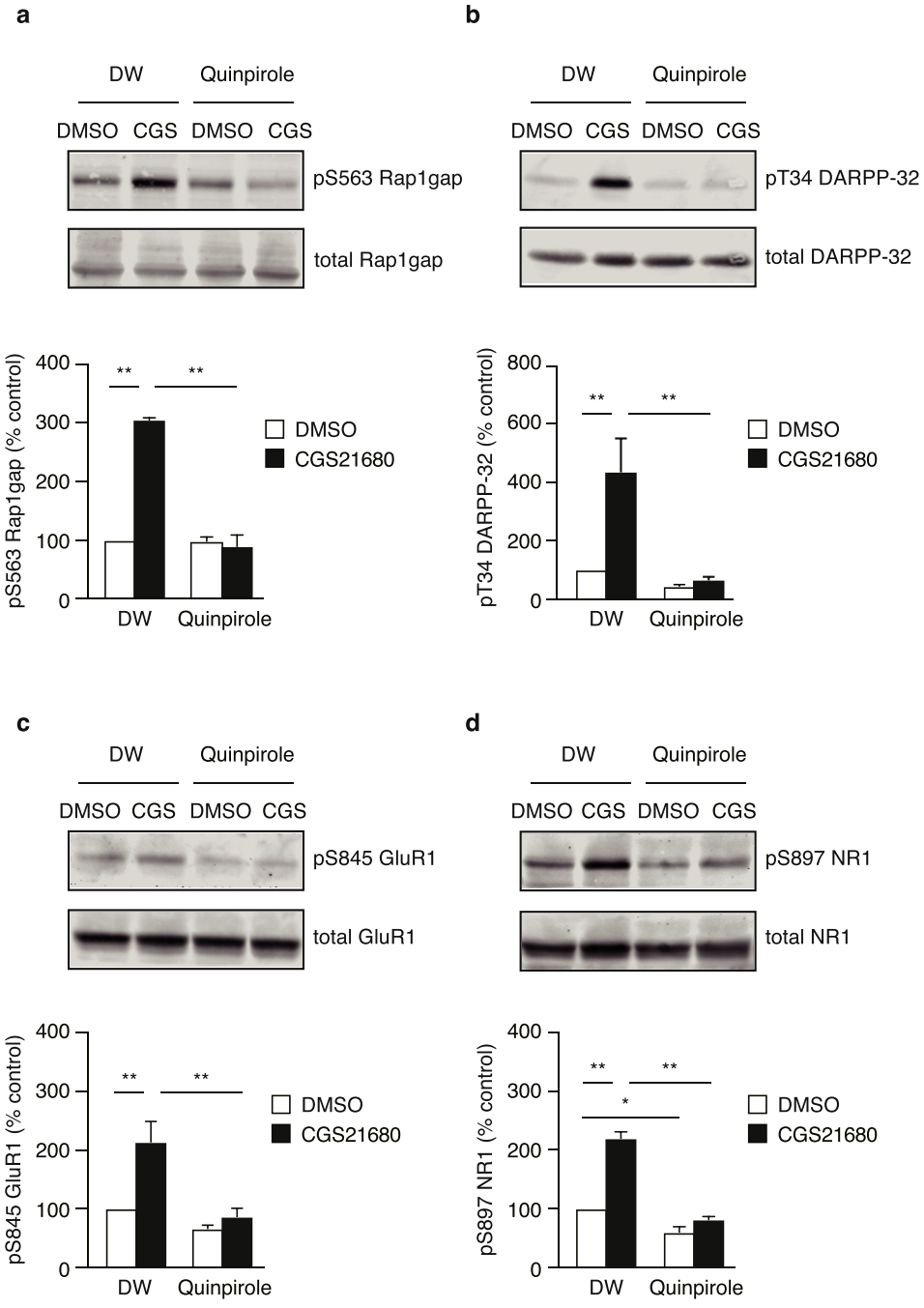

Fig. 2. Stimulation of adenosine A2AR promotes Rap1gap phosphorylation in striatal slices. Striatal slices were treated with CGS21680 (CGS) (5 μM) for 5 min after pretreatment with quinpirole (1 μM) 10 min before. The phosphorylated protein levels were determined via immunoblotting using phospho-specific antibodies. **(a)** pS563 Rap1gap. **(b)** pT34 DARPP-32. **(c)** pS845 GluR1. **(d)** pS897 NR1. The upper panels show immunoblots for phosphoproteins and the respective total proteins. Quantification of the immunoblot assay is shown in the bottom panels. The data were normalized to the total protein levels in each sample and were expressed as percentages of levels in the control slices. Data are presented as the mean ± SEM (n = 4 slices for all groups) of four independent experiments. Two-way ANOVA analysis for pS563 Rap1gap; quinpirole, $F(1,12) = 110.2$, $p < 0.0001$; CGS21680, $F(1,12) = 90.16$, $p < 0.0001$; interaction, $F(1,12) = 107.3$, $p < 0.0001$. Two-way ANOVA analysis for pT34 DARPP-32; quinpirole, $F(1,12) = 13.35$, $p = 0.0033$; CGS21680, $F(1,12) = 9.344$, $p = 0.0100$; interaction, $F(1,12) = 7.23$, $p = 0.0197$. Two-way ANOVA analysis for pS845 GluR1; quinpirole, $F(1,12) = 16.87$, $p = 0.0015$; CGS21680, $F(1,12) = 11.59$, $p = 0.0052$; interaction, $F(1,12) = 5.595$, $p = 0.0357$. Two-way ANOVA analysis for pS897 NR1; quinpirole, $F(1,12) = 134.5$, $p < 0.0001$; CGS21680, $F(1,12) = 84.28$, $p < 0.0001$; interaction, $F(1,12) = 40.75$, $p < 0.0001$. *$p < 0.05$ and **$p < 0.01$ compared with the corresponding control. Full-length blots are presented in Supplementary Fig. S7.

3.4. Inhibition of dopamine D2R promotes Rap1gap phosphorylation in the accumbal D2R-MSNs

We further investigated the effect of the A2AR agonist on Rap1gap phosphorylation *in vivo* (Fig. S4a). Treatment with CGS21680 slightly but not significantly increased the phosphorylation level of Rap1gap at S563 in the NAc of C57BL/6 mice (Fig. 4a). This may be because that the basal levels of extracellular dopamine interfere with the effect of A2AR activation towards the Rap1gap phosphorylation by acting through D2R. Therefore, we measured the phosphorylation level of Rap1gap S563 after treatment with the D2R antagonist eticlopride in mice (Fig. S4b). Treatment with eticlopride significantly increased the phosphorylation level of Rap1gap in a dose-dependent manner (Fig. 4b). Furthermore, the eticlopride-induced Rap1gap phosphorylation was detected in accumbal D2R-MSNs of *Drd2-mVenus* transgenic mice, in which D2R-MSNs express mVenus (Fig. 4c and Fig. S4c), suggesting that the basal levels of extracellular dopamine inhibit Rap1gap phosphorylation *in vivo*.

3.5. Inhibition of adenosine A2AR suppresses the Rap1gap phosphorylation promoted by the D2R antagonist

To examine the interaction between A2AR and D2R in the NAc of mice, we further investigated the effect of the A2AR antagonist SCH58261 on eticlopride-induced Rap1gap phosphorylation (Fig. S5). Pretreatment with SCH58261 significantly suppressed the Rap1gap phosphorylation induced by eticlopride treatment ($p < 0.01$, Fig. 5). SCH58261 itself had no effect on the phosphorylation level of Rap1gap. Thus, A2AR stimulation is required for the D2R antagonist-induced Rap1gap phosphorylation. Taken together, these results suggest that adenosine promotes Rap1gap phosphorylation through A2AR, but dopamine counteracts this effect through D2R in MSNs in basal conditions

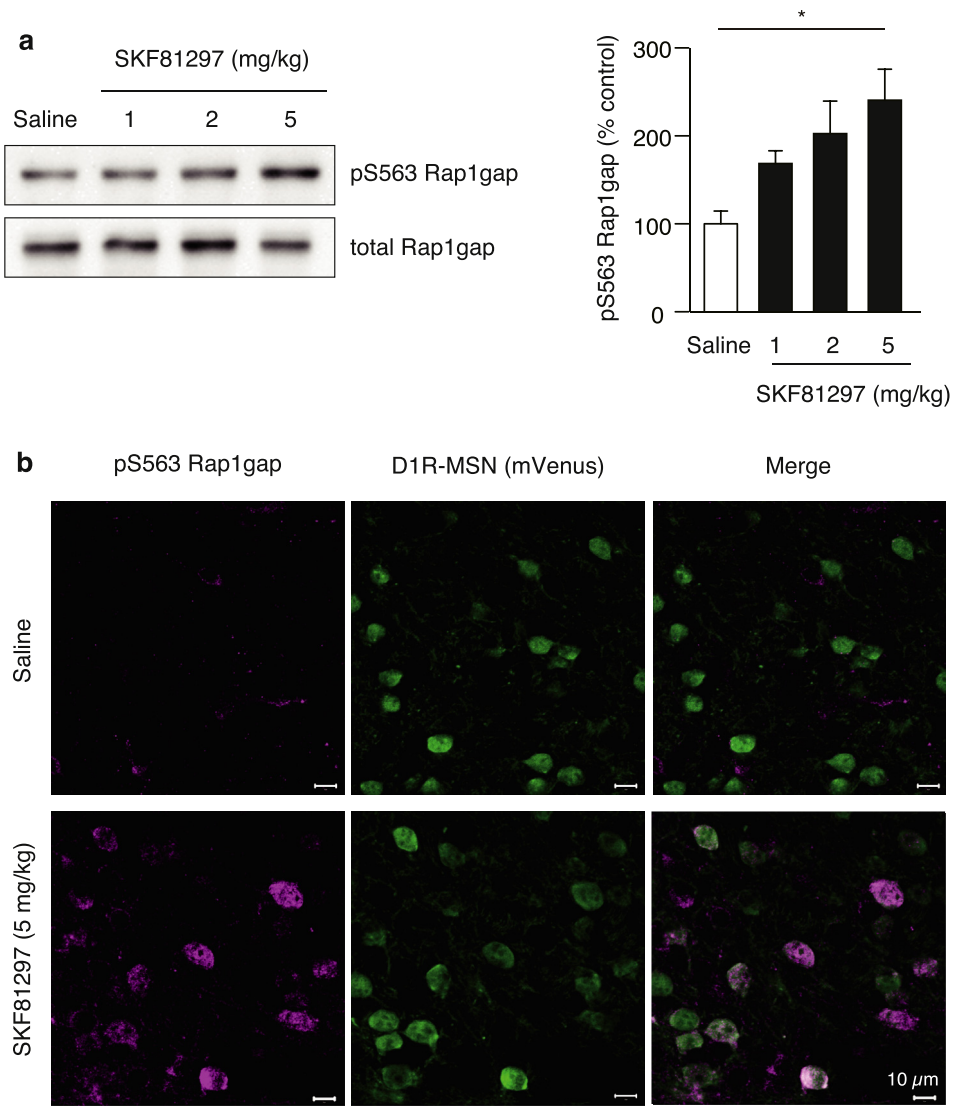

Fig. 3. Stimulation of the dopamine D1R promotes Rap1gap phosphorylation in accumbal D1R-MSNs. (a) Dopamine D1R agonist SKF81297 administration dose-dependently stimulated the phosphorylation of Rap1gap in the NAc 15 min after SKF81297 injection. Left panels show representative immunoblots. Quantification of the immunoblotting assay is shown in the right panel. Data are presented as the mean ± SEM (n = 3 mice for all groups). One-way ANOVA analysis; $F(3,8) = 4.698$, $p = 0.0356$. *$p < 0.05$. Full-length blots are presented in Supplementary Fig. S8. **(b)** Phosphorylated Rap1gap was detected in D1R-MSNs in the NAc after SKF81297 injection. *Drd1-mVenus* transgenic mice were administered saline or SKF81297 (5 mg/kg, i.p.), and immunohistochemical analysis was performed 15 min after the treatment. Immunofluorescence staining using an anti-Rap1gap antibody specific for phosphorylation at S563 (left panels) or an anti-GFP antibody (middle panels) is shown. The scale bar indicates 10 μm.

(Fig. 1a).

3.6. Mathematical model for dopamine and adenosine signals in D2R-MSNs

A mathematical model was constructed to reproduce the interaction between the dopamine and adenosine signaling pathways in D2R-MSNs. In this model, we focused on the phosphorylation level of Rap1gap because PKA-mediated Rap1gap phosphorylation is regulated by adenosine/A2AR/G_{olf}/adenylate cyclase and dopamine/D2R/G_i/adenylate cyclase pathways in D2R-MSNs. According to previous reports, the basal extracellular concentration of adenosine and dopamine is estimated at approximately 25–250 nM and 7–20 nM, respectively, in the rat brain (Dunwiddie and Masino, 2001; Chen, 2005). We found that about 10% of Rap1gap in the NAc of mice was phosphorylated at S563 under basal condition (Fig. S11). Therefore, we simulated a change of phosphorylated Rap1gap level when extracellular dopamine and/or adenosine were used within a wide range of their concentration including basal condition.

We first fixed adenosine concentration at 10, 100 or 1000 nM, and modeled the effect of extracellular dopamine level on Rap1gap phosphorylation (Fig. 6a). When the adenosine concentration was set at 10 nM, a little amount of Rap1gap was phosphorylated within a physiological range of extracellular dopamine concentration (Fig. 6a left panel). The phosphorylation level of Rap1gap was increased with reducing extracellular dopamine under the circumstances (Fig. 6a left panel). The dopamine concentration-response curve was markedly shifted toward the right depending on adenosine concentration, and the phosphorylation level of Rap1gap was slightly increased even within the physiological range of dopamine concentration (Fig. 6a middle and right panel).

We next fixed dopamine concentration at 1, 10 or 100 nM, and modeled the effect of extracellular adenosine on Rap1gap phosphorylation (Fig. 6b). When the dopamine level was kept low at 1 nM, adenosine increased the phosphorylation level of Rap1gap in a concentration-dependent manner (Fig. 6b left panel). As extracellular dopamine concentration at 10 nM (around basal level) or 100 nM, Rap1gap phosphorylation level was remarkably suppressed within the physiological range of extracellular adenosine concentration (Fig. 6b middle panel and right panel).

Finally, we integrated these mathematical models and analyzed the level of phosphorylated Rap1gap for different combination of the extracellular adenosine and dopamine concentration. The phosphorylation of Rap1gap in D2R-MSNs was promoted under the certain condition that meets both low concentration of dopamine and above basal concentration of adenosine (Fig. 6c).

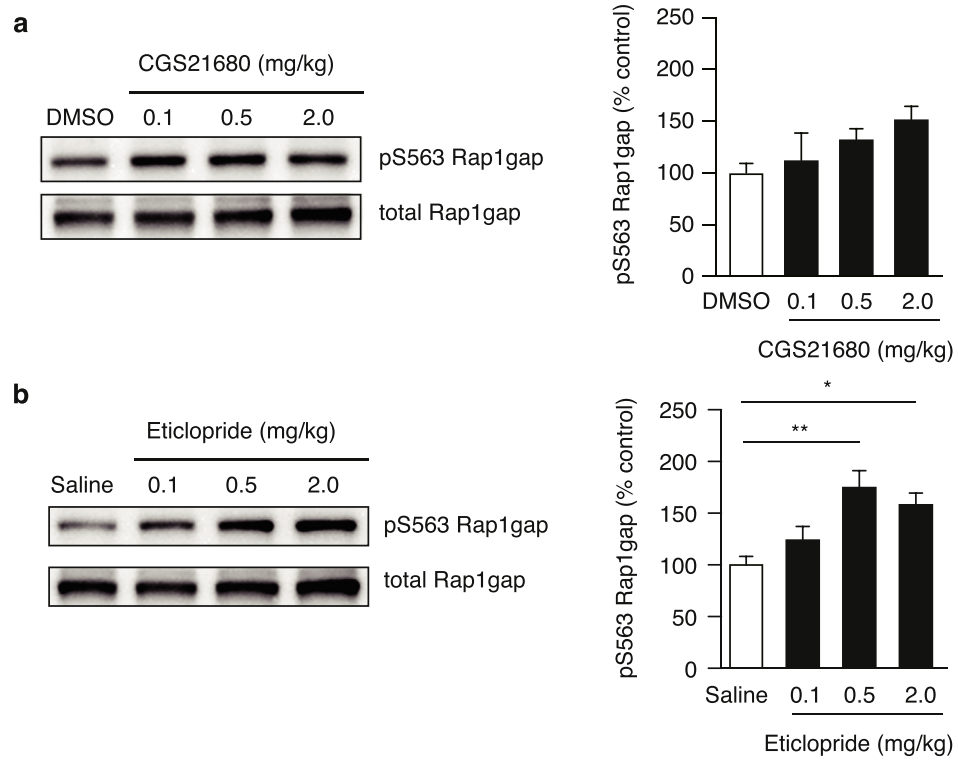

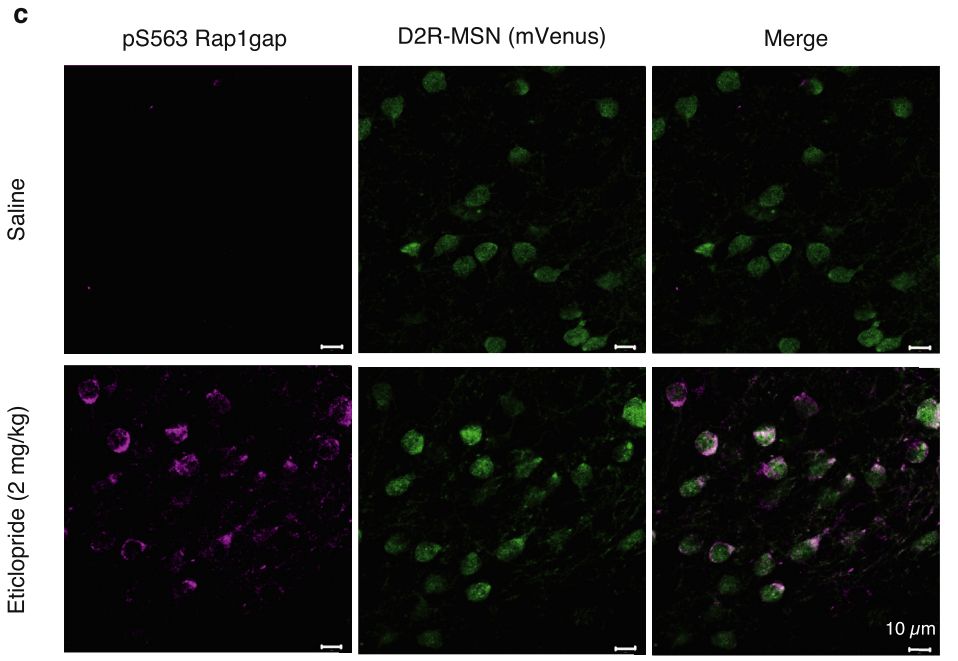

Fig. 4. Inhibition of the dopamine D2R but not adenosine A2AR stimulation promotes Rap1gap phosphorylation in the accumbal D2R-MSNs. **(a)** Adenosine A2AR agonist CGS21680 administration failed to stimulate the phosphorylation of Rap1gap in the NAc 15 min after CGS21680 injection. Left panels show representative immunoblots. Quantification of the immunoblotting assay is shown in the right panel. Data are presented as the mean ± SEM (n = 4 mice for control, CGS 0.1 and CGS 0.5, n = 5 mice for CGS 2.0). One-way ANOVA analysis; $F(3,13) = 2.234$, $p = 0.1328$. **(b)** Dopamine D2R antagonist eticlopride administration stimulated the phosphorylation of Rap1gap in the NAc 15 min after eticlopride injection. Left panels show representative immunoblots. Quantification of the immunoblotting assay is shown in the right panel. Data are presented as the mean ± SEM (n = 4 mice for control, CGS 0.1 and CGS 0.5, n = 5 mice for CGS 2.0). One-way ANOVA analysis; $F(3,13) = 6.564$, $p = 0.0061$. *$p < 0.05$ and **$p < 0.01$. Full-length blots are presented in Supplementary Fig. S9. **(c)** Phosphorylated Rap1gap was detected in D2R-MSNs in the NAc after eticlopride injection. *Drd2-mVenus* transgenic mice were administered saline or eticlopride (2 mg/kg, i.p.), and immunohistochemical analysis was performed 15 min after the treatment. Immunofluorescence staining using an anti-Rap1gap antibody specific for phosphorylation at S563 (left panels) or an anti-GFP antibody (middle panels) is shown. The scale bar indicates 10 μm.

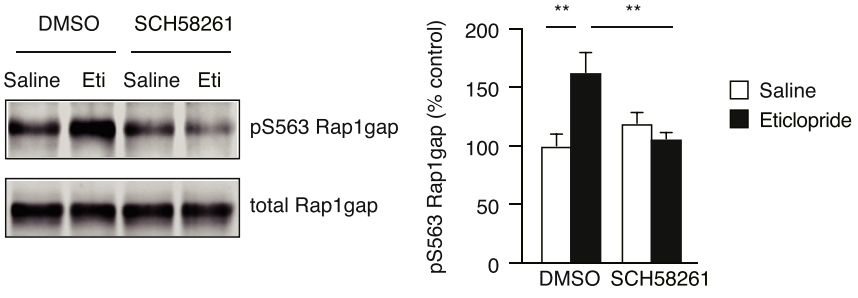

Fig. 5. Inhibition of the adenosine A2AR suppresses the Rap1gap phosphorylation promoted by the dopamine D2R antagonist. The adenosine A2AR antagonist SCH58261 (10 mg/kg) was administered 5 min before the eticlopride (Eti, 2 mg/kg) treatment. The phosphorylation of Rap1gap in the NAc was measured 15 min after eticlopride injection. Left panels show representative immunoblots. Quantification of the immunoblotting assay is shown in the right panel. Data are presented as the mean ± SEM (n = 12 mice for all groups) of four independent experiments. Two-way ANOVA analysis; eticlopride, $F(1, 43) = 4.89$, $p = 0.0324$; SCH58261, $F(1, 43) = 2.778$, $p = 0.1029$; interaction, $F(1, 43) = 11.53$, $p = 0.0015$. **$p < 0.01$. Full-length blots are presented in Supplementary Fig. S10.

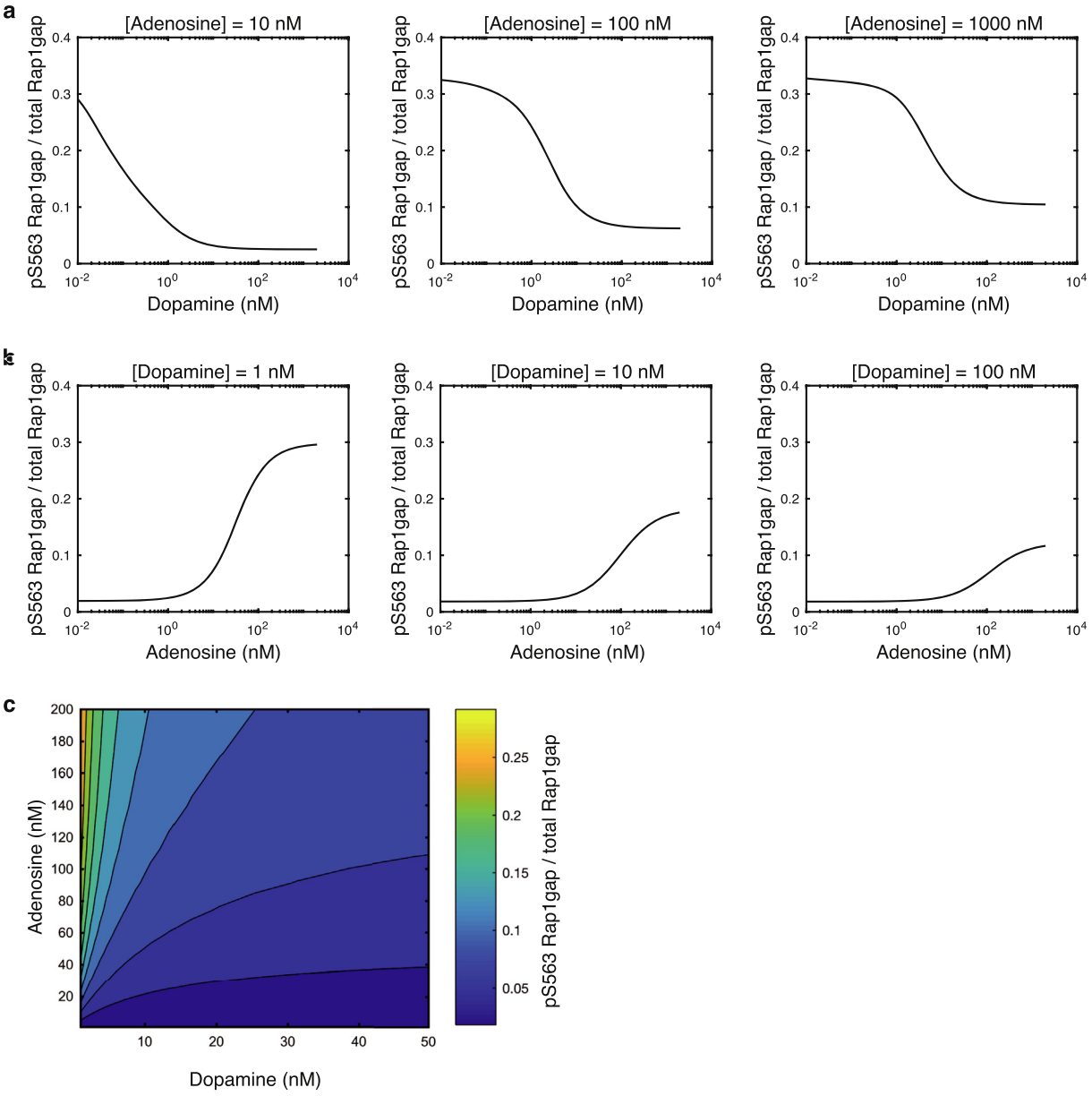

Fig. 6. Mathematical model prediction of the dopamine and adenosine dose-dependent responses of the phosphorylation of Rap1gap in D2R-MSN. (a) Dopamine dose-dependent responses of phosphorylation of Rap1gap at three different extracellular adenosine levels. Horizontal and vertical axes represent the input level of dopamine (logarithmic scale) and the ratio of phosphorylated Rap1gap S563 to the total Rap1gap. **(b)** Adenosine dose-dependent responses of phosphorylation of Rap1gap at S563 at three different extracellular dopamine levels. Horizontal and vertical axes represent the input level of adenosine (logarithmic scale) and the ratio of phosphorylated Rap1gap S563 to the total Rap1gap. **(c)** Dopamine and adenosine dose-dependent responses of phosphorylation of Rap1gap. The color indicates the phosphorylation level of Rap1gap at S563.

4. Discussion

We have recently reported that dopamine phosphorylates and activates Rasgrp2 through D1R/PKA in D1R-MSNs (Nagai et al., 2016a). Consequently, Rasgrp2-mediated Rap1 activation stimulates MAPK, which increases the excitability of D1R-MSNs to enhance reward-related behaviors (Nagai et al., 2016a). As showed in Fig. 1a, in this study, we demonstrated that D1R stimulation phosphorylated Rap1gap in D1R-MSNs (Figs. 1c and 3). Our results also showed that A2AR stimulation enhanced Rap1gap phosphorylation in striatal slice (Fig. 2a). Administration of the D2R antagonist enhanced Rap1gap phosphorylation, and this effect was blocked by pretreatment with the A2AR antagonist although A2AR agonist had minimal effect (Figs. 4 and 5). These results suggest that PKA is inactivated in D2R-MSNs in basal conditions because endogenous dopamine inhibits PKA activity *in vivo*. Adenosine can activate PKA in D2R-MSNs under the conditions of dopamine depletion or with blockade of D2R. Our results developed the interaction between D1R and A1R in D1R-MSNs and the interaction between D2R and A2AR in D2R-MSNs proposed by the analyses of DARPP-32 phosphorylation in slices and *in vivo* (Nishi et al., 1997, 2011; Lindskog et al., 1999; Yabuuchi et al., 2006).

Phosphorylation of Rap1gap at S505 and S563 has been shown to decrease its GAP activity on Rap1 (McAvoy et al., 2009). We found that about 10% of Rap1gap was phosphorylated at S563 in the NAc of saline-treated mice, and D1R agonist or D2R antagonist administration increased the phosphorylation of Rap1gap S563 approximately twice that of saline-treated mice. We believe that Rap1gap phosphorylation is effective to regulate Rap1 activity. First, we calculated the change of Rap1gap S563 phosphorylation in the NAc including both D1R-MSNs and D2R-MSNs. If D1R agonist induced 2-fold increase of Rap1gap S563

phosphorylation in the NAc, Rap1gap S563 phosphorylation in D1R-MSNs should be increased 3 times the basal level whereas Rap1gap S563 phosphorylation was unchanged in D2R-MSNs. Second, it is possible that there are several phosphorylation sites including S505 and S563 in Rap1gap-C-terminal that can be phosphorylated by PKA since S563 phosphorylation occupied 20% of Rap1gap-C-terminal phosphorylation under basal condition (Fig. S11d). Third, as Rap1 activity is regulated by both GEF and GAP simultaneously, we assume that PKA phosphorylates Rasgrp2 to promote Rap1 activation and, meanwhile, phosphorylates Rap1gap to inhibit Rap1 inactivation. Based on these points, Rap1 is efficiently activated through these two signaling pathways in D1R-MSNs or D2R-MSNs, thereby activating the Rap1/MAPKK/MAPK signaling pathway.

The extracellular dopamine concentration is changed dynamically and rapidly in the striatum released from dopaminergic neurons in response to stimuli (Robinson et al., 2002; Wenzel et al., 2015; Collins et al., 2016). D1R and D2R have low and high affinity sites for dopamine (Seeman et al., 2006; Seeman, 2007; Marcellino et al., 2012), and the high affinity sites of both receptors are thought to play more crucial role than low affinity site. Since the Kd values of high affinity site of D1R and D2R are around 200 nM and 10 nM, respectively (Marcellino et al., 2012), extracellular dopamine seems to bind to D2R rather than D1R under basal condition. Adenosine is produced both intracellularly and extracellularly from breakdown of adenine nucleotides including ATP and ADP (Latini and Pedata, 2001). Intracellularly produced adenosine is transported to the extracellular region through a nucleoside transporter (King et al., 2006). Although there are many different adenosine sources, striatal A2AR is activated by ecto-5′-nucleotidase (CD73)-mediated ATP-derived adenosine (Augusto et al., 2013; Ena et al., 2013), which accounts for tonic A2AR activation. According to pharmacological approaches or microdialysis analyses in the rat brain, basal adenosine concentrations are estimated to be in the range of 25–250 nM (Dunwiddie and Masino, 2001). The affinity of A1R and A2AR is around 100 nM (Dunwiddie and Masino, 2001). Therefore, basal extracellular adenosine concentrations are sufficient to tonically activate A1R and A2AR. Taking these matters into account, we simulated a change of phosphorylated Rap1gap level downstream A2AR and high affinity D2R in D2R-MSNs. We assumed that PKA was activated at low concentration of dopamine and inactivated at high concentration of dopamine in D2R-MSNs when basal adenosine was present (Fig. 6). This observation was consistent with the experimental findings *in vivo* (Figs. 4 and 5). Although we did not simulate mathematical models of the Rap1gap phosphorylation downstream of A1R and high affinity D1R in D1R-MSNs, PKA activity may be controlled in D1R-MSNs in the opposite way, which means that PKA is inactivated at low concentration of dopamine and activated at high concentration. Thus, when basal adenosine is present, the switch between the D1R-MSN and D2R-MSN activation states occurs efficiently depending on the concentration of extracellular dopamine (Fig. 7).

In the present study, we focused on the direct antagonism of A2AR signaling and D2R signaling in MSN. Regarding this antagonism, there are two other possibilities that D2R antagonist could indirectly enhance A2AR signaling by increasing adenosine release and that A2AR antagonist could indirectly enhance D2R signaling by increasing dopamine release. The former possibility cannot be denied since no studies have examined the effect of D2R antagonist on adenosine release yet. However, the latter possibility could be excluded by the previous findings that systemic or intra-striatal administration of A2AR antagonist has no effect on the extracellular level of dopamine (Dremencov et al., 2017; Golembiowska and Dziubina, 2004).

Recently, the concept of A2AR-D2R heteromerization has been highlighted, which proposes that A2AR-D2R interactions include not only at the level of adenylate cyclase, but also multiple allosteric interactions (Ferre et al., 2011; Navarro et al., 2014; Bonaventura et al., 2015). In addition to D2R-MSN, A2AR is also expressed in glutamatergic terminals (Rodrigues et al., 2005) and cholinergic interneurons (Preston et al., 2000) to regulate neurotransmitters release in the striatum, including glutamate and acetylcholine (Schiffmann et al., 2007). These neurotransmitters also control basal ganglia circuits and contribute to striatal function. Furthermore, extracellular adenosine is known to dynamically change especially in pathological conditions (Dunwiddie and Masino, 2001; Cunha, 2016; Dale and Frenguelli, 2009). The above facts cannot be ignored to propose a fine-tuned model of D2R-A2AR interactions at the level of adenylate cyclase. However, in this study, we proposed a simplified mathematic model based on the perspective of classical pharmacology to clarify how dopamine and adenosine co-operatively regulate PKA activity in the D2R-MSNs.

D2R antagonists are commonly used as pharmacotherapy for schizophrenia, and A2A antagonists are used as pharmacotherapy for Parkinson's disease (Kapur and Remington, 2001; Jenner, 2005; Seeman, 2013; Pinna, 2014). Although the location of the target receptors of these drugs in the brain is well investigated, how and where these drugs act at the cellular and molecular level remain largely unknown. This has been the major obstacle for developing new therapeutic drugs. Here, we found that the D2R antagonist activated PKA and induced Rap1gap phosphorylation in D2R-MSNs (Fig. 4b and c). The effects of D2R antagonists can be examined at cellular and molecular levels through monitoring Rap1gap phosphorylation not only by immunoblotting but also by immunohistochemistry. Furthermore, the effects of A2AR antagonists could be evaluated in combination with D2R antagonists (Fig. 5). We propose that examining the mode of actions of the existing drugs at cellular and molecular levels using these approaches is important and may also be useful in the development of new drugs.

5. Conclusions

The current study demonstrated cell-type specific PKA activation to regulate Rap1gap phosphorylation. These findings indicate that PKA/Rap1 pathway contributes not only in D1R-MSNs but also in D2R-MSNs. Consequently, we propose a model that explains how the active state shifts between D1R-MSNs and D2R-MSNs (Fig. 7). Basal dopamine concentration cannot activate D1R but activate D2R to suppress D2R-MSN activity. High dopamine concentration can activate D1R to activate D1R-MSN, and activate D2R to suppress D2R-MSN activity. Low dopamine concentration can activate neither D1R nor D2R so that D2R-MSN becomes active without D2R's suppression and because basal adenosine tonically activates A2AR. In conclusion, with the cooperation of adenosine, dopamine concentration plays a role of switch in controlling active state shift between D1R-MSNs and D2R-MSNs in the neural circuit.

Conflicts of interest

The authors declare no conflict of interest.

Acknowledgments

We thank Dr. Kazuto Kobayashi for providing *Drd1-mVenus/Drd2-mVenus* transgenic mice. We thank Drs. Akinori Nishi and Md. Hasanuzzaman Shohag for technical advice. We wish to acknowledge Sachi Kozawa, Miki Taguchi, Division for Medical Research Engineering and Division of Experimental Animals at Nagoya University Graduate School of Medicine for technical assistance. We also thank Takako Ishii for secretarial assistance. This work was supported by the following funding sources: “Bioinformatics for Brain Sciences” performed under the SRPBS from MEXT and AMED, “Brain/MINDS” from AMED, JSPS KAKENHI Grant Number [17J10615], [17H01380], [17H02220], [15K06772], [17K19483], [16K18393], MEXT KAKENHI Grant Number [17H05561] and Joint Research by the National Institutes of Natural Sciences, Grant number [01111706].

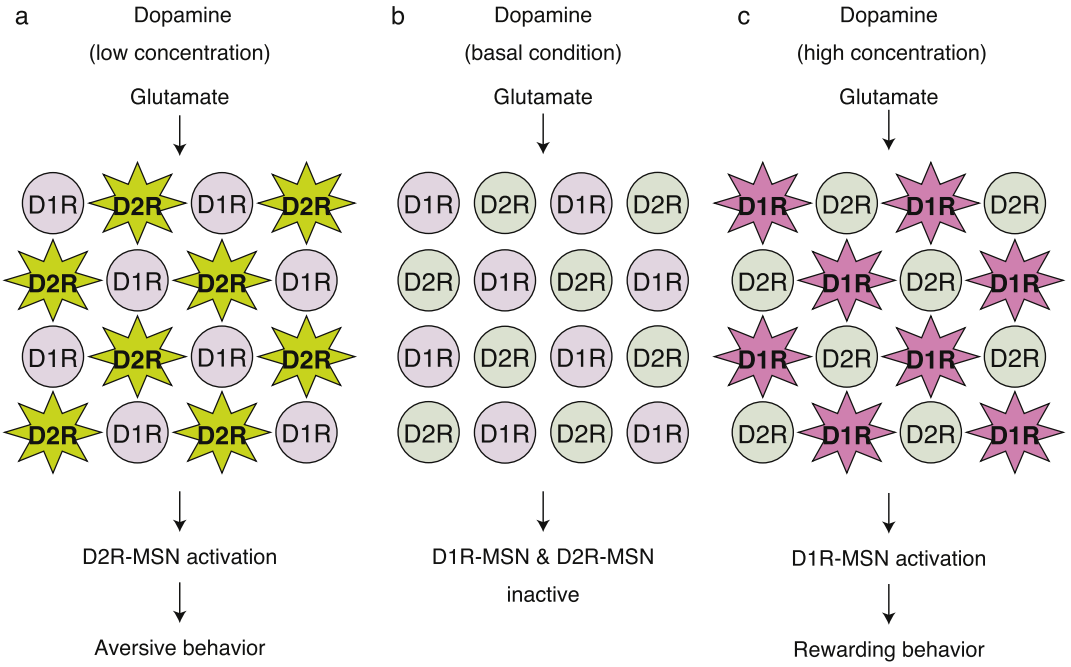

Fig. 7. Working model: Switch between the D1R-MSN and D2R-MSN activation states occurs efficiently depending on the concentration of dopamine. (a) When dopamine concentration is low, D2R-MSNs show high excitability that facilitates glutamate stimulation and are activated, consequently leading to aversive behavior. In pathophysiological condition, the dopamine hypofunctional state may be associated with Parkinson' disease, attention deficit hyperactivity disorder and restless legs syndrome. **(b)** When dopamine concentration is in basal condition, both D1R-MSNs and D2R-MSNs show low excitability and are inactive. **(c)** When dopamine concentration is high, D1R-MSNs show high excitability that facilitates glutamate stimulation and are activated, consequently leading to rewarding behavior. In pathophysiological condition, the dopamine hyperfunctional state may be associated with schizophrenia and drug addiction.

Appendix A. Supplementary data

Supplementary data to this article can be found online at https://doi.org/10.1016/j.neuint.2018.10.008.

References

Allen, R., 2004. Dopamine and iron in the pathophysiology of restless legs syndrome (RLS). Sleep Med. 5, 385–391.

Augusto, E., Matos, M., Sevigny, J., El-Tayeb, A., Bynoe, M.S., Muller, C.E., Cunha, R.A., Chen, J.F., 2013. Ecto-5'-nucleotidase (CD73)-mediated formation of adenosine is critical for the striatal adenosine A_{2A} receptor functions. J. Neurosci. 33, 11390–11399.

Beaulieu, J.M., Gainetdinov, R.R., 2011. The physiology, signaling, and pharmacology of dopamine receptors. Pharmacol. Rev. 63, 182–217.

Bonaventura, J., Navarro, G., Casado-Anguera, V., Azdad, K., Rea, W., Moreno, E., Brugarolas, M., Mallol, J., Canela, E.I., Lluis, C., Cortes, A., Volkow, N.D., Schiffmann, S.N., Ferre, S., Casado, V., 2015. Allosteric interactions between agonists and antagonists within the adenosine A_{2A} receptor-dopamine D_2 receptor heterotetramer. Proc. Natl. Acad. Sci. U. S. A. 112, E3609–E3618.

Chen, K.C., 2005. Evidence on extracellular dopamine level in rat striatum: implications for the validity of quantitative microdialysis. J. Neurochem. 92, 46–58.

Collins, A.L., Greenfield, V.Y., Bye, J.K., Linker, K.E., Wang, A.S., Wassum, K.M., 2016. Dynamic mesolimbic dopamine signaling during action sequence learning and expectation violation. Sci. Rep. 6, 20231.

Cunha, R.A., 2016. How does adenosine control neuronal dysfunction and neurodegeneration? J. Neurochem. 139, 1019–1055.

Dale, N., Frenguelli, B.G., 2009. Release of adenosine and ATP during ischemia and epilepsy. Curr. Neuropharmacol. 7, 160–179.

Dremencov, E., Lacinova, L., Flik, G., Folgering, J.H., Cremers, T.I., Westerink, B.H., 2017. Purinergic regulation of brain catecholamine neurotransmission: in vivo electrophysiology and microdialysis study in rats. Gen. Physiol. Biophys. 36, 431–441.

Dunwiddie, T.V., Masino, S.A., 2001. The role and regulation of adenosine in the central nervous system. Annu. Rev. Neurosci. 24, 31–55.

Ena, S.L., De Backer, J.F., Schiffmann, S.N., de Kerchove d'Exaerde, A., 2013. FACS array profiling identifies Ecto-5' nucleotidase as a striatopallidal neuron-specific gene involved in striatal-dependent learning. J. Neurosci. 33, 8794–8809.

Esteban, J.A., Shi, S.H., Wilson, C., Nuriya, M., Huganir, R.L., Malinow, R., 2003. PKA phosphorylation of AMPA receptor subunits controls synaptic trafficking underlying plasticity. Nat. Neurosci. 6, 136–143.

Ferre, S., O'Connor, W.T., Svenningsson, P., Bjorklund, L., Lindberg, J., Tinner, B., Stromberg, I., Goldstein, M., Ogren, S.O., Ungerstedt, U., Fredholm, B.B., Fuxe, K., 1996. Dopamine D1 receptor-mediated facilitation of GABAergic neurotransmission in the rat strioentopenduncular pathway and its modulation by adenosine A1 receptor-mediated mechanisms. Eur. J. Neurosci. 8, 1545–1553.

Ferre, S., Quiroz, C., Orru, M., Guitart, X., Navarro, G., Cortes, A., Casado, V., Canela, E.I., Lluis, C., Franco, R., 2011. Adenosine A_{2A} receptors and A_{2A} receptor heteromers as key players in striatal function. Front. Neuroanat. 5, 36.

Fink, J.S., Weaver, D.R., Rivkees, S.A., Peterfreund, R.A., Pollack, A.E., Adler, E.M., Reppert, S.M., 1992. Molecular cloning of the rat A2 adenosine receptor: selective co-expression with D2 dopamine receptors in rat striatum. Brain Res Mol Brain Res 14, 186–195.

Fredholm, B.B., Arslan, G., Halldner, L., Kull, B., Schulte, G., Wasserman, W., 2000. Structure and function of adenosine receptors and their genes. Naunyn-Schmiedeberg's Arch. Pharmacol. 362, 364–374.

Gerfen, C.R., Engber, T.M., Mahan, L.C., Susel, Z., Chase, T.N., Monsma Jr., F.J., Sibley, D.R., 1990. D1 and D2 dopamine receptor-regulated gene expression of striatonigral and striatopallidal neurons. Science 250, 1429–1432.

Gerfen, C.R., Surmeier, D.J., 2011. Modulation of striatal projection systems by dopamine. Annu. Rev. Neurosci. 34, 441–466.

Golembiowska, K., Dziubina, A., 2004. Striatal adenosine A_{2A} receptor blockade increases extracellular dopamine release following l-DOPA administration in intact and dopamine-denervated rats. Neuropharmacology 47, 414–426.

Goto, A., Nakahara, I., Yamaguchi, T., Kamioka, Y., Sumiyama, K., Matsuda, M., Nakanishi, S., Funabiki, K., 2015. Circuit-dependent striatal PKA and ERK signaling underlies rapid behavioral shift in mating reaction of male mice. Proc. Natl. Acad. Sci. U. S. A. 112, 6718–6723.

Hallett, P.J., Spoelgen, R., Hyman, B.T., Standaert, D.G., Dunah, A.W., 2006. Dopamine D1 activation potentiates striatal NMDA receptors by tyrosine phosphorylation-dependent subunit trafficking. J. Neurosci. 26, 4690–4700.

Hamaguchi, T., Nakamuta, S., Funahashi, Y., Takano, T., Nishioka, T., Shohag, M.H., Yura, Y., Kaibuchi, K., Amano, M., 2015. In vivo screening for substrates of protein kinase A using a combination of proteomic approaches and pharmacological modulation of kinase activity. Cell Struct. Funct. 40, 1–12.

Herve, D., Le Moine, C., Corvol, J.C., Belluscio, L., Ledent, C., Fienberg, A.A., Jaber, M., Studler, J.M., Girault, J.A., 2001. $G\alpha_{olf}$ levels are regulated by receptor usage and control dopamine and adenosine action in the striatum. J. Neurosci. 21, 4390–4399.

Herve, D., Levi-Strauss, M., Marey-Semper, I., Verney, C., Tassin, J.P., Glowinski, J., Girault, J.A., 1993. G_{olf} and G_s in rat basal ganglia: possible involvement of G_{olf} in the coupling of dopamine D1 receptor with adenylyl cyclase. J. Neurosci. 13, 2237–2248.

Hikida, T., Kimura, K., Wada, N., Funabiki, K., Nakanishi, S., 2010. Distinct roles of synaptic transmission in direct and indirect striatal pathways to reward and aversive behavior. Neuron 66, 896–907.

Hoops, S., Sahle, S., Gauges, R., Lee, C., Pahle, J., Simus, N., Singhal, M., Xu, L., Mendes, P., Kummer, U., 2006. COPASI–a COmplex PAthway SImulator. Bioinformatics 22, 3067–3074.

Iversen, S.D., Iversen, L.L., 2007. Dopamine: 50 years in perspective. Trends Neurosci. 30, 188–193.

Jenner, P., 2005. Istradefylline, a novel adenosine A_{2A} receptor antagonist, for the treatment of Parkinson's disease. Expet Opin. Invest. Drugs 14, 729–738.
Kapur, S., Remington, G., 2001. Dopamine D_2 receptors and their role in atypical antipsychotic action: still necessary and may even be sufficient. Biol. Psychiatry 50, 873–883.
Kato, K., Yazawa, T., Taki, K., Mori, K., Wang, S., Nishioka, T., Hamaguchi, T., Itoh, T., Takenawa, T., Kataoka, C., Matsuura, Y., Amano, M., Murohara, T., Kaibuchi, K., 2012. The inositol 5-phosphatase SHIP2 is an effector of RhoA and is involved in cell polarity and migration. Mol. Biol. Cell 23, 2593–2604.
Kemp, J.M., Powell, T.P., 1971. The structure of the caudate nucleus of the cat: light and electron microscopy. Philos. Trans. R. Soc. Lond. B Biol. Sci. 262, 383–401.
King, A.E., Ackley, M.A., Cass, C.E., Young, J.D., Baldwin, S.A., 2006. Nucleoside transporters: from scavengers to novel therapeutic targets. Trends Pharmacol. Sci. 27, 416–425.
Kull, B., Svenningsson, P., Fredholm, B.B., 2000. Adenosine A_{2A} receptors are colocalized with and activate G_{olf} in rat striatum. Mol. Pharmacol. 58, 771–777.
Kuroda, K., Yamada, S., Tanaka, M., Iizuka, M., Yano, H., Mori, D., Tsuboi, D., Nishioka, T., Namba, T., Iizuka, Y., Kubota, S., Nagai, T., Ibi, D., Wang, R., Enomoto, A., Isotani-Sakakibara, M., Asai, N., Kimura, K., Kiyonari, H., Abe, T., Mizoguchi, A., Sokabe, M., Takahashi, M., Yamada, K., Kaibuchi, K., 2011. Behavioral alterations associated with targeted disruption of exons 2 and 3 of the Disc1 gene in the mouse. Hum. Mol. Genet. 20, 4666–4683.
Latini, S., Pedata, F., 2001. Adenosine in the central nervous system: release mechanisms and extracellular concentrations. J. Neurochem. 79, 463–484.
Lindskog, M., Svenningsson, P., Fredholm, B.B., Greengard, P., Fisone, G., 1999. Activation of dopamine D2 receptors decreases DARPP-32 phosphorylation in striatonigral and striatopallidal projection neurons via different mechanisms. Neuroscience 88, 1005–1008.
Marcellino, D., Kehr, J., Agnati, L.F., Fuxe, K., 2012. Increased affinity of dopamine for D_2-like versus D_1-like receptors. Relevance for volume transmission in interpreting PET findings. Synapse 66, 196–203.
McAvoy, T., Zhou, M.M., Greengard, P., Nairn, A.C., 2009. Phosphorylation of Rap1GAP, a striatally enriched protein, by protein kinase A controls Rap1 activity and dendritic spine morphology. Proc. Natl. Acad. Sci. U. S. A. 106, 3531–3536.
Montmayeur, J.P., Guiramand, J., Borrelli, E., 1993. Preferential coupling between dopamine D2 receptors and G-proteins. Mol. Endocrinol. 7, 161–170.
Morgan, J.M., McCormack, D.G., Griffiths, M.J., Morgan, C.J., Barnes, P.J., Evans, T.W., 1991. Adenosine as a vasodilator in primary pulmonary hypertension. Circulation 84, 1145–1149.
Nagai, T., Nakamuta, S., Kuroda, K., Nakauchi, S., Nishioka, T., Takano, T., Zhang, X., Tsuboi, D., Funahashi, Y., Nakano, T., Yoshimoto, J., Kobayashi, K., Uchigashima, M., Watanabe, M., Miura, M., Nishi, A., Kobayashi, K., Yamada, K., Amano, M., Kaibuchi, K., 2016a. Phosphoproteomics of the dopamine pathway enables discovery of Rap1 activation as a reward signal in vivo. Neuron 89, 550–565.
Nagai, T., Yoshimoto, J., Kannon, T., Kuroda, K., Kaibuchi, K., 2016b. Phosphorylation signals in striatal medium spiny neurons. Trends Pharmacol. Sci. 37, 858–871.
Nair, A.G., Gutierrez-Arenas, O., Eriksson, O., Vincent, P., Hellgren Kotaleski, J., 2015. Sensing positive versus negative reward signals through adenylyl cyclase-coupled GPCRs in direct and indirect pathway striatal medium spiny neurons. J. Neurosci. 35, 14017–14030.
Nakano, T., Doi, T., Yoshimoto, J., Doya, K., 2010. A kinetic model of dopamine- and calcium-dependent striatal synaptic plasticity. PLoS Comput. Biol. 6, e1000670.
Navarro, G., Aguinaga, D., Moreno, E., Hradsky, J., Reddy, P.P., Cortes, A., Mallol, J., Casado, V., Mikhaylova, M., Kreutz, M.R., Lluis, C., Canela, E.I., McCormick, P.J., Ferre, S., 2014. Intracellular calcium levels determine differential modulation of allosteric interactions within G protein-coupled receptor heteromers. Chem. Biol. (Lond.) 21, 1546–1556.
Nishi, A., Kuroiwa, M., Shuto, T., 2011. Mechanisms for the modulation of dopamine D_1 receptor signaling in striatal neurons. Front. Neuroanat. 5, 43.
Nishi, A., Snyder, G.L., Greengard, P., 1997. Bidirectional regulation of DARPP-32 phosphorylation by dopamine. J. Neurosci. 17, 8147–8155.
Pascoli, V., Terrier, J., Hiver, A., Luscher, C., 2015. Sufficiency of mesolimbic dopamine neuron stimulation for the progression to addiction. Neuron 88, 1054–1066.
Pinna, A., 2014. Adenosine A_{2A} receptor antagonists in Parkinson's disease: progress in clinical trials from the newly approved istradefylline to drugs in early development and those already discontinued. CNS Drugs 28, 455–474.
Porkka-Heiskanen, T., Alanko, L., Kalinchuk, A., Stenberg, D., 2002. Adenosine and sleep. Sleep Med. Rev. 6, 321–332.
Preston, Z., Lee, K., Widdowson, L., Freeman, T.C., Dixon, A.K., Richardson, P.J., 2000. Adenosine receptor expression and function in rat striatal cholinergic interneurons. Br. J. Pharmacol. 130, 886–890.
Richardson, P.J., Kase, H., Jenner, P.G., 1997. Adenosine A_{2A} receptor antagonists as new agents for the treatment of Parkinson's disease. Trends Pharmacol. Sci. 18, 338–344.
Robinson, D.L., Heien, M.L., Wightman, R.M., 2002. Frequency of dopamine concentration transients increases in dorsal and ventral striatum of male rats during introduction of conspecifics. J. Neurosci. 22, 10477–10486.
Rodrigues, R.J., Alfaro, T.M., Rebola, N., Oliveira, C.R., Cunha, R.A., 2005. Co-localization and functional interaction between adenosine A_{2A} and metabotropic group 5 receptors in glutamatergic nerve terminals of the rat striatum. J. Neurochem. 92, 433–441.
Schiffmann, S.N., Fisone, G., Moresco, R., Cunha, R.A., Ferre, S., 2007. Adenosine A_{2A} receptors and basal ganglia physiology. Prog. Neurobiol. 83, 277–292.
Seeman, P., 2007. Antiparkinson therapeutic potencies correlate with their affinities at dopamine $D2^{High}$ receptors. Synapse 61, 1013–1018.
Seeman, P., 2013. Schizophrenia and dopamine receptors. Eur. Neuropsychopharmacol 23, 999–1009.
Seeman, P., Schwarz, J., Chen, J.F., Szechtman, H., Perreault, M., McKnight, G.S., Roder, J.C., Quirion, R., Boksa, P., Srivastava, L.K., Yanai, K., Weinshenker, D., Sumiyoshi, T., 2006. Psychosis pathways converge via $D2^{high}$ dopamine receptors. Synapse 60, 319–346.
Shohamy, D., 2011. Learning and motivation in the human striatum. Curr. Opin. Neurobiol. 21, 408–414.
Snyder, G.L., Allen, P.B., Fienberg, A.A., Valle, C.G., Huganir, R.L., Nairn, A.C., Greengard, P., 2000. Regulation of phosphorylation of the GluR1 AMPA receptor in the neostriatum by dopamine and psychostimulants in vivo. J. Neurosci. 20, 4480–4488.
Southan, C., Sharman, J.L., Benson, H.E., Faccenda, E., Pawson, A.J., Alexander, S.P., Buneman, O.P., Davenport, A.P., McGrath, J.C., Peters, J.A., Spedding, M., Catterall, W.A., Fabbro, D., Davies, J.A., 2016. The IUPHAR/BPS Guide to PHARMACOLOGY in 2016: towards curated quantitative interactions between 1300 protein targets and 6000 ligands. Nucleic Acids Res. 44, D1054–D1068.
Svenningsson, P., Lindskog, M., Ledent, C., Parmentier, M., Greengard, P., Fredholm, B.B., Fisone, G., 2000. Regulation of the phosphorylation of the dopamine- and cAMP-regulated phosphoprotein of 32 kDa in vivo by dopamine D_1, dopamine D_2, and adenosine A_{2A} receptors. Proc. Natl. Acad. Sci. U. S. A. 97, 1856–1860.
Tingley, W.G., Ehlers, M.D., Kameyama, K., Doherty, C., Ptak, J.B., Riley, C.T., Huganir, R.L., 1997. Characterization of protein kinase A and protein kinase C phosphorylation of the N-methyl-D-aspartate receptor NR1 subunit using phosphorylation site-specific antibodies. J. Biol. Chem. 272, 5157–5166.
Walaas, S.I., Aswad, D.W., Greengard, P., 1983. A dopamine- and cyclic AMP-regulated phosphoprotein enriched in dopamine-innervated brain regions. Nature 301, 69–71.
Wardas, J., 2002. Neuroprotective role of adenosine in the CNS. Pol. J. Pharmacol. 54, 313–326.
Wenzel, J.M., Rauscher, N.A., Cheer, J.F., Oleson, E.B., 2015. A role for phasic dopamine release within the nucleus accumbens in encoding aversion: a review of the neurochemical literature. ACS Chem. Neurosci. 6, 16–26.
Wise, R.A., 2004. Dopamine, learning and motivation. Nat. Rev. Neurosci. 5, 483–494.
Yabuuchi, K., Kuroiwa, M., Shuto, T., Sotogaku, N., Snyder, G.L., Higashi, H., Tanaka, M., Greengard, P., Nishi, A., 2006. Role of adenosine A1 receptors in the modulation of dopamine D1 and adenosine A2A receptor signaling in the neostriatum. Neuroscience 141, 19–25.